INTERNATIONAL JOURNAL OF
NUMERICAL ANALYSIS AND MODELING
Volume 11, Number 4, Pages 762–786

FINITE VOLUME MULTILEVEL APPROXIMATION OF THE SHALLOW WATER EQUATIONS WITH A TIME EXPLICIT SCHEME

ARTHUR BOUSQUET, MARTINE MARION, AND ROGER TEMAM

Abstract. We consider a simple advection equation in space dimension one and the linearized shallow water equations in space dimension two and describe and implement two different multilevel finite volume discretizations in the context of the utilization of the incremental methods with time explicit or semi-explicit schemes.

Key words. finite volume methods, multilevel methods, Euler explicit schemes, shallow water equations, stability analysis.

1. Introduction

This article is related to the article [5] in which we investigated multilevel finite volume discretizations for the one dimensional advection equation and for the one and two-dimensional linear shallow water equations. This article is also related to the article [2] in which we presented and implemented a hierarchical multilevel finite volume discretization for the shallow water equations combined with a Runge-Kutta discretization of order four in time. The article [5] focused on the Euler implicit time discretization, this article continues with the stability analysis of the multilevel finite volume methods but with a partly or fully Euler explicit discretization in time.

We consider the simple one-dimensional advection equation and the full two-dimensional shallow water equations without viscosity, linearized around a constant flow. For the shallow water equations the boundary conditions and the analysis depend on the nature of the background flow; see [13] and below. In this article we choose the supercritical case which allows us to use a classical upwind finite volume scheme, see e.g. [14].

Our motivations are two-fold. On the physical side the shallow water equations are a simplified model of the Primitive Equations (PEs) of the atmosphere and the oceans. As shown in [21], [18], in a rectangular geometry, the PEs can be expanded using a certain vertical modal decomposition; with such a decomposition we obtain an infinite system of coupled equations which resemble the shallow water equations. See e.g. [8], [9] for the actual numerical resolution of these coupled systems. However it appears in these articles that the problems to be solved are very difficult (demanding) and performant numerical methods are needed to tackle more and more realistic problems. We turned in [2] to multilevel finite volume methods which are here our second motivation. Finite volume methods are desirable for the treatment of complicated geometrical domains such as the oceans, and multilevel methods of the incremental unknown type are useful for the implementation of multilevel methods. Such methods have been introduced in the context of the Nonlinear Galerkin Method in [15] (see also [16]), in the context of finite

Received by the editors November 28, 2013.
2000 *Mathematics Subject Classification.* 35R35, 49J40, 60G40.
This research was supported by NSF Grant DMS 1206438, and by the Research Fund of Indiana University.

differences in [20], and in the context of spectral methods and turbulence in [11]. In continuation of [2], this article explores the finite volume implementation of the incremental unknowns.

Considering, for simplicity, a rectangular geometry, we divide our domain in "small" cells of size Δx for the one dimensional case and of size $\Delta x \times \Delta y$ for the two dimensional case which we combine at the first level of increment, in coarse cells of size $3\Delta x$ and $3\Delta x \times 3\Delta y$ respectively. The unknowns on the small cells are the original unknowns denoted by u or $\mathbf{u}$, and we also introduce, for the coarse cells, suitable averaged values of the unknowns denoted by U or $\mathbf{U}$. We also introduce the incremental unknowns, denoted by Z or $\mathbf{Z}$, which are frozen during the computation on the coarse mesh and which allow us to go from the unknowns on the coarse mesh to the unknowns on the fine mesh.

We apply different time steps on the fine mesh and on the coarse mesh. Since the cells are smaller on the fine mesh we use a smaller time step, $\Delta t/p$, where p is chosen, and we use a time step Δt for our computation on the coarse mesh. This coarsening can be repeated once more considering cells of size $9\Delta x$ or $9\Delta x \times 9\Delta y$, and possibly several times as the programming is repetitive and its cost is thus small; however as done in [5] we restrict ourselves in this article to one coarsening.

The stability analysis developed here is done on a multilevel method that is different than that presented in [2] and closer to that presented in [5] (see however below and in Section 5). At the end of this article we numerically compare the method presented in this article with the averaged multilevel method used in [2] and [5].

Of course there is a very rich literature on the discretization of the shallow water equations using multilevel and/or parallel methods; see e.g. [1], [3], [10], [12], [17], [22], and the references therein.

This article is organized as follows. In Section 2 we present the hierarchical multilevel discretization for the one dimensional advection equation. For the time discretization we use the Euler explicit or semi-explicit method. Then in Section 3 we investigate a hierarchical multilevel discretization for the two dimensional linear shallow water equations. In Section 4 we re-introduce the Averaged Multilevel Finite Volume method presented in [2] and [5] for the advection equation. We discuss several questions related to the stability of the method that we also investigate numerically. Finally, we present some numerical results on the two dimensional linear shallow water equations comparing computations done solely on the fine grid, computations only done on the coarse mesh and computations done with the hierarchical multilevel method and the averaged multilevel method.

2. Hierarchical Multilevel Finite Volume Method I

We present in this section a hierarchical multilevel method using a finite volume discretization (HFVM) for the following advection equation on the one-dimensional domain $\mathcal{M} = (0, L)$:

$$\frac{\partial u}{\partial t}(x,t) + \frac{\partial u}{\partial x}(x,t) = 0, \quad x \in \mathcal{M}, \quad t > 0. \tag{1}$$

This equation is supplemented with the boundary condition

$$u(0,t) = 0, \quad t > 0, \tag{2}$$

and the initial condition

$$u(x,0) = u^0(x), \quad x \in \mathcal{M}, \tag{3}$$

where $u^0 \in L^2(\mathcal{M})$ is given.

2.1. Multilevel spatial discretization. We introduce, on the interval $\mathcal{M}$, a mesh consisting of $3N$ cells $(k_i)_{1\leq i\leq 3N}$ of uniform length Δx with $3N\Delta x = L$. For $i = 0, \ldots, 3N$, we set

$$x_{i+1/2} = i\Delta x,$$

so that

$$k_i = (x_{i-1/2}, x_{i+1/2}).$$

We also consider the center of each cell:

$$x_i = \frac{x_{i-1/2} + x_{i+1/2}}{2} = (i-1)\Delta x + \frac{\Delta x}{2}, \ \ 1 \leq i \leq 3N.$$

The discrete unknowns will be denoted by u_i, $1 \leq i \leq 3N$, and are expected to be some approximation of the mean value of u over k_i. By integrating equation (1) over k_i we obtain:

$$\frac{d}{dt}\int_{k_i} u(x,t)dx + u(x_{i+1/2},t) - u(x_{i-1/2},t) = 0.$$

Here the term $u(x_{i+1/2},t)$ will be approximated by $u_i(t)$ using an "upwind" scheme due to the direction of the characteristics for equation (1). The upwind finite volume discretization reads

$$\frac{du_i}{dt}(t) + \frac{u_i(t) - u_{i-1}(t)}{\Delta x} = 0, \ \ 1 \leq i \leq 3N, \tag{4}$$

where we have set, in view of (2)

$$u_0(t) = 0. \tag{5}$$

These equations are supplemented with the initial conditions

$$u_i(0) = \frac{1}{\Delta x}\int_{k_i} u^0(x)dx, \ 1 \leq i \leq 3N. \tag{6}$$

Let us now introduce a coarser mesh consisting of the intervals K_l, $1 \leq l \leq N$, with length $3\Delta x$ obtained as follows

$$K_l = k_{3l-2} \cup k_{3l-1} \cup k_{3l}{}^1 = (x_{3l-2-1/2}, x_{3l+1/2}). \tag{7}$$

Let $(u_i)_{1\leq i\leq 3N}$ denote as above the spatial approximation of u on the fine mesh $(k_i)_{1\leq i\leq 3N}$. Then one of the possible approximations of u on the coarse mesh is given by

$$U_l = \frac{1}{3}\left[u_{3l-2} + u_{3l-1} + u_{3l}\right], \ 1 \leq l \leq N, \tag{8}$$

and we can introduce the incremental unknowns

$$\left\{\begin{array}{l} Z_{3l-2} = u_{3l-2} - U_l, \\ Z_{3l-1} = u_{3l-1} - U_l, \\ Z_{3l} = u_{3l} - U_l. \end{array}\right. \tag{9}$$

We observe that $\sum_{\alpha=0}^{2} Z_{3l-\alpha} = 0$, and by inverting the system (8)-(9), we see that for $1 \leq l \leq N$,

$$\left\{\begin{array}{l} u_{3l-2} = U_l + Z_{3l-2} \\ u_{3l-1} = U_l - Z_{3l-2} - Z_{3l} \\ u_{3l} = U_l + Z_{3l} \end{array}\right. \tag{10}$$

[1]Including, strictly speaking, the separation points.

At this point the unknowns on the fine grid are decomposed as the sum of the terms $(U_l)_{1\leq l\leq N}$ associated with the coarse grid and increments $(Z_i)_{1\leq i\leq 3N}$ associated with the fine grid, as in (10).

With this in mind, we consider a coarse grid discretization of the equation similar to (4), that reads :

$$\frac{dU_l}{dt}(t)+\frac{U_l(t)-U_{l-1}(t)}{3\Delta x}=0,\ \ 1\leq l\leq N. \tag{11}$$

2.2. Fully explicit Euler discretization in time and stability analysis. Let us now introduce some time step Δt. We will discretize equation (4) on the finer mesh by using some smaller time step $\Delta t/p$, with $p>1$ and equation (11) on the coarser mesh by using the time step Δt. For both equations we will use the explicit Euler scheme so that we will call this multilevel scheme fully explicit.

More precisely let $p>1$ and $q>1$ be two fixed integers. Our multi-step discretization consists in alternating p steps of (4) with time step $\Delta t/p$ and q steps of (11) with time step Δt, during which the incremental unknowns Z_i are frozen. Then using equations (10) we can go back to the finer mesh and perform p iterations on this mesh, etc.

The approximate solutions are recursively defined as follows. We start with the sequence u_i^0 given by

$$u_i^0=\frac{1}{\Delta x}\int_{k_i}u^0(x)dx\ \text{ for } 1\leq i\leq N, \tag{12}$$

where u^0 is our initial condition, see (3).

Then we proceed by induction, suppose that n is a multiple of $(q+1)$ and the $(u_i^n)_{1\leq i\leq 3N}$ are known. Here u_i^n is an approximation of the mean value of u over k_i at time $t_n=n\Delta t$. For $0\leq r\leq p$ we introduce the discrete times $t_{n+r/p}=t_n+r\Delta t/p$ and the corresponding unknowns $u_i^{n+r/p}$. They are determined by the following discretization of (4)-(5) using the explicit Euler scheme :

$$\begin{cases}\dfrac{p}{\Delta t}(u_i^{n+(r+1)/p}-u_i^{n+r/p})+\dfrac{1}{\Delta x}(u_i^{n+r/p}-u_{i-1}^{n+r/p})=0,\\ u_0^{n+(r+1)/p}=0.\end{cases} \tag{13}$$

Here $1\leq i\leq 3N$ and $0\leq r\leq p-1$. Note that after p iterations the approximations u_i^{n+1} at time $t_{n+1}=(n+1)\Delta t$ are now defined.

Before describing the iterations on the coarser mesh let us investigate the stability of the above scheme. It is convenient to introduce the step functions $u_h^{n+r/p}$ defined for $0\leq r\leq p$ by:

$$u_h^{n+r/p}(x)=u_i^{n+r/p},\ x\in k_i,\ 1\leq i\leq 3N,$$

whose L^2 norm is denoted by $|u_h^{n+r/p}|$. We first observe that

$$\begin{aligned}|u_h^0|^2=\sum_{i=1}^N\Delta x|u_i^0|^2&=\sum_{i=1}^N\Delta x\left(\frac{1}{\Delta x}\int_{k_i}u^0(x)dx\right)^2\\ &\leq\ \text{by the Cauchy-Schwarz inequality}\\ &\leq\sum_{i=1}^N\int_{k_i}u^0(x)^2dx=|u^0|^2.\end{aligned} \tag{14}$$

By multiplying (13) by $2\frac{\Delta t}{p}\Delta x\ u_i^{n+r/p}$ and adding the corresponding equalities for $i = 1, ..., 3N$, we obtain

$$\begin{aligned} &2\Delta x \sum_{i=1}^{3N} (u_i^{n+(r+1)/p} - u_i^{n+r/p})\ u_i^{n+r/p} \\ &+2(\Delta t/p) \sum_{i=1}^{3N} (u_i^{n+r/p} - u_{i-1}^{n+r/p})\ u_i^{n+r/p} = 0. \end{aligned} \tag{15}$$

For the first term in (15) we have

$$\begin{aligned} 2(u_i^{n+(r+1)/p} - u_i^{n+r/p})\ u_i^{n+r/p} = |u_i^{n+(r+1)/p}|^2 - |u_i^{n+r/p}|^2 \\ -|u_i^{n+(r+1)/p} - u_i^{n+r/p}|^2 \end{aligned} \tag{16}$$

and by taking the sum for $i = 1, .., 3N$ we are left with

$$\begin{aligned} 2\Delta x \sum_{i=1}^{3N} (u_i^{n+(r+1)/p} - u_i^{n+r/p})\ u_i^{n+r/p} = |u_h^{n+(r+1)/p}|^2 - |u_h^{n+r/p}|^2 \\ -\Delta x \sum_{i=1}^{3N} |u_i^{n+(r+1)/p} - u_i^{n+r/p}|^2. \end{aligned}$$

Then for the second term in (15), since

$$2(u_i^{n+r/p} - u_{i-1}^{n+r/p})\ u_i^{n+r/p} = |u_i^{n+r/p}|^2 - |u_{i-1}^{n+r/p}|^2 + |u_i^{n+r/p} - u_{i-1}^{n+r/p}|^2, \tag{17}$$

we see that

$$2\sum_{i=1}^{3N} (u_i^{n+r/p} - u_{i-1}^{n+r/p}) u_i^{n+r/p} = |u_{3N}^{n+r/p}|^2 + \sum_{i=1}^{3N} |u_i^{n+r/p} - u_{i-1}^{n+r/p}|^2. \tag{18}$$

Hence we infer from (15) that

$$\begin{aligned} |u_h^{n+(r+1)/p}|^2 + (\Delta t/p)|u_{3N}^{n+r/p}|^2 + (\Delta t/p) \sum_{i=1}^{3N} |u_i^{n+r/p} - u_{i-1}^{n+r/p}|^2 \\ -\Delta x \sum_{i=1}^{3N} |u_i^{n+(r+1)/p} - u_i^{n+r/p}|^2 = |u_h^{n+r/p}|^2. \end{aligned} \tag{19}$$

Now we have to estimate the term $|u_i^{n+(r+1)/p} - u_i^{n+r/p}|^2$ which appears with the negative sign in the left-hand side of (19). From equation (13) we have

$$u_i^{n+(r+1)/p} - u_i^{n+r/p} = -\frac{\Delta t}{p}\frac{1}{\Delta x}(u_i^{n+r/p} - u_{i-1}^{n+r/p}).$$

Therefore, the last two terms in the right hand-side of (19) can be rewritten as

$$\begin{aligned} (\Delta t/p) \sum_{i=1}^{3N} |u_i^{n+r/p} - u_{i-1}^{n+r/p}|^2 - \Delta x \sum_{i=1}^{3N} |u_i^{n+(r+1)/p} - u_i^{n+r/p}|^2 \\ = \frac{\Delta t}{p}\left[1 - \frac{\Delta t}{p}\frac{1}{\Delta x}\right] \sum_{i=1}^{3N} |u_i^{n+r/p} - u_{i-1}^{n+r/p}|^2 \end{aligned}$$

so that (19) yields :

(20)
$$|u_h^{n+(r+1)/p}|^2 + (\Delta t/p)|u_{3N}^{n+r/p}|^2 + \frac{\Delta t}{p}\left[1 - \frac{\Delta t}{p}\frac{1}{\Delta x}\right]\sum_{i=1}^{3N}|u_i^{n+r/p} - u_{i-1}^{n+r/p}|^2 = |u_h^{n+r/p}|^2.$$

Therefore provided the following CFL condition is satisfied:

$$\frac{\Delta t}{p} \leq \Delta x, \tag{21}$$

we infer from (20) that

$$|u_h^{n+(r+1)/p}| \leq |u_h^{n+r/p}|, \;\; 0 \leq r \leq p-1. \tag{22}$$

As already noticed, after the p iterations on the fine grid, the approximation u_h^{n+1} at time $t_{n+1} = (n+1)\Delta t$ is now determined and in view of (22) written for $r = p-1, ..., 0$, it satisfies

$$|u_h^{n+1}| \leq |u_h^n|. \tag{23}$$

We will now perform q iterations on the coarse mesh using the large time step Δt and the spatial decomposition (10). In (10) at time $t_{n+m} = (n+m)\Delta t$, $2 \leq m \leq q+1$ the incremental unknowns Z are frozen at time $(n+1)\Delta t$ so that our approximations will take the form

$$u_{3l-\alpha}^{n+m} = U_l^{n+m} + Z_{3l-\alpha}^{n+1}, \;\; 1 \leq l \leq N, \;\; \alpha = 0, 1, 2. \tag{24}$$

Here, U_l^{n+1} is given through definition (8)

$$U_l^{n+1} = \frac{1}{3}\left[u_{3l-2}^{n+1} + u_{3l-1}^{n+1} + u_{3l}^{n+1}\right], \; 1 \leq l \leq N,$$

and

$$Z_{3l-\alpha}^{n+1} = u_{3l-\alpha}^{n+1} - U_l^{n+1}.$$

Then U_l^{n+m}, $2 \leq m \leq q+1$, is defined by discretizing (11) using the explicit Euler scheme. Hence the U_l^{n+m+1} are recursively defined, for $m = 1, \ldots, q-1$, starting from U_l^{n+1} and given by:

$$\begin{cases} \dfrac{U_l^{n+m+1} - U_l^{n+m}}{\Delta t} + \dfrac{U_l^{n+m} - U_{l-1}^{n+m}}{3\Delta x} = 0, \quad 1 \leq l \leq N, \\ U_0^{n+m+1} = 0. \end{cases} \tag{25}$$

Note that (25) is somehow the analog of (13) on the coarse grid. Consequently, similarly to the calculations above, by multiplying equation (25) by $6\Delta x \Delta t U_l^{n+m}$ and adding the resulting equalities for $l = 1, ..., N$, we obtain :

$$|U_{3h}^{n+m+1}|^2 + \Delta t|U_N^{n+m}|^2 + \Delta t\left[1 - \frac{\Delta t}{3\Delta x}\right]\sum_{l=1}^{N}|U_l^{n+m} - U_{l-1}^{n+m}|^2 = |U_{3h}^{n+m}|^2. \tag{26}$$

Here, U_{3h}^{n+m} is the step function which takes the value U_l^{n+m} on K_l.

Therefore, assuming the CFL condition,

$$\frac{\Delta t}{3\Delta x} \leq 1, \tag{27}$$

we infer from (26) that

$$|U_{3h}^{n+m+1}|^2 \leq |U_{3h}^{n+m}|^2. \tag{28}$$

Recall that the approximate solution is given by (24). Now, since

$$\sum_{\alpha=0}^{2} Z_{3l-\alpha}^{n+1} = 0, \tag{29}$$

we have :

$$\sum_{\alpha=0}^{2} |u_{3l-\alpha}^{n+m}|^2 = \sum_{\alpha=0}^{2} |U_l^{n+m} + Z_{3l-\alpha}^{n+1}|^2 = 3|U_l^{n+m}|^2 + \sum_{\alpha=0}^{2} |Z_{3l-\alpha}^{n+1}|^2. \tag{30}$$

This yields readily the following equality for the L^2 norms of the corresponding step functions:

$$|u_h^{n+m}|^2 = |U_{3h}^{n+m}|^2 + |Z_h^{n+1}|^2, \tag{31}$$

that indicates that, in some sense, the coarse component U_{3h}^{n+m} and the increment Z_h^{n+1} are L^2-orthogonal. In view of (31), by adding $|Z_h^{n+1}|^2$ to both sides of the inequality (28), we conclude that :

$$|u_h^{n+m}| \leq |u_h^{n+1}|, \;\; 1 \leq m \leq q. \tag{32}$$

Altogether the inequalities (22), (23) and (32) provide the stability of the multilevel method when the CFL conditions (21) and (27) hold true. In summary we have proven the following result.

Theorem 2.1. *The multilevel scheme defined by equations* (13) *and* (24)-(25) *is stable in* $L^\infty(0,+\infty,L^2(\mathcal{M}))$ *provided the following CFL condition is satisfied:*

$$\frac{\Delta t}{\Delta x} \leq \min(3,p). \tag{33}$$

More precisely, for all n *and* $s \geq 0$*, the following bounds hold true*

$$\begin{aligned} &|u_h^n| \leq |u^0|, \\ &|u_h^{s(q+1)+r/p}| \leq |u^0|, \text{ for } r = 1, \cdots, p. \end{aligned} \tag{34}$$

Remark 2.1. *We note that for* $p = 1, 2$ *the CFL condition* (27) *on the coarser mesh is less restrictive than the one on the fine mesh* (21)*. For* $p = 3$ *the two conditions are the same, while for* $p > 3$ *the CFL condition is more restrictive on the coarse mesh. Therefore a possible alternative is to use an Euler implicit scheme on the fine mesh and an Euler explicit scheme on the coarse mesh, a case which we now describe.*

2.3. An implicit/explicit Euler multilevel scheme. Following Remark 2.1 we discuss now a variant of our scheme based on an Euler implicit time discretization on the fine mesh and an Euler explicit discretization on the coarse mesh.

The new equation equations on the fine mesh now read (compare to (13)) :

$$\begin{cases} \dfrac{p}{\Delta t}\left(u_i^{n+(r+1)/p} - u_i^{n+r/p}\right) + \dfrac{1}{\Delta x}\left(u_i^{n+(r+1)/p} - u_{i-1}^{n+(r+1)/p}\right) = 0, \\ \\ u_0^{n+(r+1)/p} = 0, \end{cases} \tag{35}$$

for $1 \leq i \leq 3N$, $0 \leq r \leq p-1$.

In order to estimate the L^2 norm of the corresponding step function $u_h^{n+(r+1)/p}$, let us multiply (35) with $2\frac{\Delta t}{p}\Delta x \; u_i^{n+(r+1)/p}$ and add the corresponding equalities

for $i = 1, ..., 3N$. This provides readily :

$$|u_h^{n+(r+1)/p}|^2 - |u_h^{n+r/p}|^2 + |u_h^{n+(r+1)/p} - u_h^{n+r/p}|^2 + \frac{\Delta t}{p}\left[|u_{3N}^{n+(r+1)/p}|^2 + \sum_{i=1}^{3N} |u_i^{n+(r+1)/p} - u_{i-1}^{n+(r+1)/p}|^2\right] = 0, \tag{36}$$

so that

$$|u_h^{n+(r+1)/p}| \leq |u_h^{n+r/p}|, \tag{37}$$

and :

$$|u_h^{n+1}| \leq |u_h^{n+r/p}| \leq |u_h^n|, \;\; 1 \leq r \leq p. \tag{38}$$

On the coarse grid our discretization still uses the Euler Explicit scheme with the time step Δt, that is equations (24)-(25). From the previous section we know that provided the following CFL condition is enforced,

$$\frac{\Delta t}{3\Delta x} \leq 1, \tag{39}$$

the following estimates hold true

$$|u_h^{n+m}| \leq |u_h^{n+1}|, \;\; 1 \leq m \leq q. \tag{40}$$

Therefore we have obtained the following stability result.

Theorem 2.2. *The multilevel scheme defined by equations* (35) *and* (24)-(25) *is stable in* $L^\infty(0, +\infty, L^2(\mathcal{M}))$ *provided the following CFL condition is satisfied:*

$$\frac{\Delta t}{3\Delta x} \leq 1. \tag{41}$$

More precisely, for all n *and* $s \geq 0$*, the following bounds hold true*

$$\begin{aligned} &|u_h^n| \leq |u^0|, \\ &|u_h^{s(q+1)+r/p}| \leq |u^0|, \text{ for } r = 1, \cdots, p. \end{aligned} \tag{42}$$

3. Hierarchical Multilevel Finite Volume Method II

We now want to extend our multilevel finite volume method to the more complex case of the Shallow Water equations linearized around a constant flow $(\tilde{u}_0, \tilde{v}_0, \tilde{\phi}_0)$ (see equations (44) below). The boundary conditions which can be associated with these equations depend on the relative values of the velocities $(\tilde{u}_0^2, \tilde{v}_0^2 >$ or $< g\tilde{\phi}_0)$, that is whether these velocities are sub- or supercritical (sub- or supersonic). We consider here the supercritical case where

$$\tilde{\phi}_0 > 0, \quad \tilde{u}_0 > \sqrt{g\tilde{\phi}_0}, \;\; \tilde{v}_0 > \sqrt{g\tilde{\phi}_0}. \tag{43}$$

More work on finite volumes for the supercritical and subcritical cases can be found in [4].

3.1. The equations. We consider the domain $\mathcal{M} = (0, L_1) \times (0, L_2)$ and the system

$$\left\{ \begin{array}{l} \dfrac{\partial u}{\partial t} + \tilde{u}_0 \dfrac{\partial u}{\partial x} + \tilde{v}_0 \dfrac{\partial u}{\partial y} + g\dfrac{\partial \phi}{\partial x} = 0, \\ \dfrac{\partial v}{\partial t} + \tilde{u}_0 \dfrac{\partial v}{\partial x} + \tilde{v}_0 \dfrac{\partial v}{\partial y} + g\dfrac{\partial \phi}{\partial y} = 0, \\ \dfrac{\partial \phi}{\partial t} + \tilde{u}_0 \dfrac{\partial \phi}{\partial x} + \tilde{v}_0 \dfrac{\partial \phi}{\partial y} + \tilde{\phi}_0 \left(\dfrac{\partial u}{\partial x} + \dfrac{\partial v}{\partial y}\right) = 0. \end{array} \right. \tag{44}$$

Here (u, v) is the horizontal velocity and ϕ is the fluid depth over the bottom. The advecting velocities $\tilde{u}_0$, $\tilde{v}_0$ and the mean height $\tilde{\phi}_0$ are supposed to be constants and positive. For the supercritical flow under consideration we supplement (44) with the boundary conditions:

$$u = v = \phi = 0 \text{ at } \{x = 0\} \cup \{y = 0\} \tag{45}$$

and the initial conditions

$$(u, v, \phi) = (u^0, v^0, \phi^0) \text{ at } t = 0. \tag{46}$$

Here (u^0, v^0, ϕ^0) is given in $\mathbf{H} = L^2(\mathcal{M})^3$.

To rewrite this system in a more compact form let us introduce the vectorial unknown $\mathbf{u} = (u, v, \phi)$ and the operator $\mathbf{Au} = (A_1\mathbf{u}, A_2\mathbf{u}, A_3\mathbf{u})$ given by

$$\begin{aligned} A_1\mathbf{u} &= \tilde{u}_0\frac{\partial u}{\partial x} + \tilde{v}_0\frac{\partial u}{\partial y} + g\frac{\partial \phi}{\partial x}, \\ A_2\mathbf{u} &= \tilde{u}_0\frac{\partial v}{\partial x} + \tilde{v}_0\frac{\partial v}{\partial y} + g\frac{\partial \phi}{\partial y}, \\ A_3\mathbf{u} &= \tilde{u}_0\frac{\partial \phi}{\partial x} + \tilde{v}_0\frac{\partial \phi}{\partial y} + \tilde{\phi}_0\left(\frac{\partial u}{\partial x} + \frac{\partial v}{\partial y}\right). \end{aligned} \tag{47}$$

With these notations, (44) is rewritten in the form

$$\frac{d\mathbf{u}}{dt} + \mathbf{Au} = 0. \tag{48}$$

Under the assumption (43), the operator $\mathbf{A}$ has positivity properties. Indeed let us equip $\mathbf{H}$ with the following scalar product :

$$\langle \mathbf{u}, \mathbf{u}' \rangle = (u, u') + (v, v') + \frac{g}{\tilde{\phi}_0}(\phi, \phi'), \tag{49}$$

for $\mathbf{u} = (u, v, \phi)$ and $\mathbf{u}' = (u', v', \phi')$ where $(.,.)$ denotes the standard scalar product on $L^2(\mathcal{M})$. We will denote by $|.|$ the associated norm. We define $D(\mathbf{A})$ as

$$D(\mathbf{A}) = \left\{\mathbf{u} \in (L^2(\mathcal{M}))^3,\ \ \mathbf{Au} \in (L^2(\mathcal{M}))^3,\ \ \mathbf{u} = 0 \text{ at } x = 0 \text{ and } y = 0\right\}. \tag{50}$$

Then for $\mathbf{u} \in D(\mathbf{A})$, we have

$$\langle \mathbf{Au}, \mathbf{u} \rangle \geq 0. \tag{51}$$

We refer the reader to [5] for the proof of this result and to [13] for the study of the boundary and initial value problem (44)-(46).

3.2. Spatial discretization. We introduce a mesh on $\mathcal{M}$ consisting of $9N_1N_2$ cells $(k_{i,j})_{1\leq i\leq 3N_1, 1\leq j\leq 3N_2}$ with $3N_1\Delta x = L_1$ and $3N_2\Delta x = L_2$ given by:

$$k_{i,j} = ((i-1)\Delta x, i\Delta x) \times ((j-1)\Delta y, j\Delta y),\ \ 1 \leq i \leq 3N_1, 1 \leq j \leq 3N_2. \tag{52}$$

Also to take into account the boundary conditions it is convenient to introduce the fictitious cells:

$$\begin{aligned} k_{0,j} &= (-\Delta x, 0) \times ((j-1)\Delta y, j\Delta y),\ \ 1 \leq j \leq 3N_2, \\ k_{i,0} &= ((i-1)\Delta x, i\Delta x) \times (-\Delta y, 0),\ \ 1 \leq i \leq 3N_1. \end{aligned} \tag{53}$$

Let us set

$$\begin{aligned} V_h = \ \{&\text{step functions } w \text{ constant on } \ k_{i,j},\ 0 \leq i \leq 3N_1, 0 \leq j \leq 3N_2 \text{ with} \\ &w_{|k_{i,j}} = w_{i,j} \text{ and } w_{0,j} = w_{i,0} = 0\} \end{aligned}$$

and $\mathbf{V}_h = (V_h)^3$.

In order to define the discrete analog of $\mathbf{A}$, let us consider the following finite difference operators on $k_{i,j}$, for $1 \leq i \leq 3N_1$, $1 \leq j \leq 3N_2$:

$$(\delta_h^1 u_h)_{i,j} = \frac{1}{\Delta x}(u_{i,j} - u_{i-1,j}),\ (\delta_h^2 u_h)_{i,j} = \frac{1}{\Delta y}(u_{i,j} - u_{i,j-1}). \tag{54}$$

Then we introduce :

$$\mathbf{A}_h \mathbf{u}_h = (A_{1h}\mathbf{u}_h, A_{2h}\mathbf{u}_h, A_{3h}\mathbf{u}_h),\ \ \mathbf{u}_h \in \mathbf{V}_h, \tag{55}$$

where A_{1h}, A_{2h} and A_{3h} are the following discrete versions of A_1, A_2 and A_3 :

$$\begin{aligned} A_{1h}\mathbf{u}_h &= \tilde{u}_0 \delta_h^1 u_h + \tilde{v}_0 \delta_h^2 u_h + g\delta_h^1 \phi_h, \\ A_{2h}\mathbf{u}_h &= \tilde{u}_0 \delta_h^1 v_h + \tilde{v}_0 \delta_h^2 v_h + g\delta_h^2 \phi_h, \\ A_{3h}\mathbf{u}_h &= \tilde{u}_0 \delta_h^1 \phi_h + \tilde{v}_0 \delta_h^2 \phi_h + \tilde{\phi}_0(\delta_h^1 u_h + \delta_h^2 v_h). \end{aligned} \tag{56}$$

Then under assumption (43), it can be shown that the operator $\mathbf{A}_h$ is positive on $\mathbf{V}_h$. The following more precise result holds true (see [5] for the proof) :

Lemma 3.1. *Under assumption* (43)*, there exists a constant* κ_1 *depending only on* $\tilde{u}_0$*,* $\tilde{v}_0$*,* $\tilde{\phi}_0$*, and* g *(and in particular on the positive numbers* $\tilde{u}_0^2 - g\tilde{\phi}_0, \tilde{v}_0^2 - g\tilde{\phi}_0$*) such that for every* $h > 0$ *and* $\mathbf{u}_h \in \mathbf{V}_h$ *:*

$$\begin{aligned} \langle \mathbf{A}_h \mathbf{u}_h, \mathbf{u}_h \rangle \ &\geq \kappa_1 \Delta y \sum_{j=1}^{3N_2} \left[|\mathbf{u}_{3N_1,j}|^2 + \sum_{i=1}^{3N_1} |\mathbf{u}_{i,j} - \mathbf{u}_{i-1,j}|^2 \right] \\ &+ \kappa_1 \Delta x \sum_{i=1}^{3N_1} \left[|\mathbf{u}_{i,3N_2}|^2 + \sum_{j=1}^{3N_2} |\mathbf{u}_{i,j} - \mathbf{u}_{i,j-1}|^2 \right]. \end{aligned} \tag{57}$$

The following estimate will also be useful in the sequel.

Lemma 3.2. *There exists a constant* κ_2 *depending only on* $\tilde{u}_0, \tilde{v}_0, \tilde{\phi}_0$*, and* g *such that for every* $h > 0$ *and* $\mathbf{u}_h \in \mathbf{V}_h$ *:*

$$|\mathbf{A}_h \mathbf{u}_h|^2 \leq \kappa_2 \sum_{i=1}^{3N_1} \sum_{j=1}^{3N_2} \left[\frac{\Delta y}{\Delta x} |\mathbf{u}_{i,j} - \mathbf{u}_{i-1,j}|^2 + \frac{\Delta x}{\Delta y} |\mathbf{u}_{i,j} - \mathbf{u}_{i,j-1}|^2 \right]. \tag{58}$$

Proof. Let $\mathbf{u}_h \in \mathbf{V}_h$. Going back to the definitions (55)-(56) and using the inequality

$$(x_1 + x_2 + ... + x_k)^2 \leq k(x_1^2 + x_2^2 + ... + x_k^2),$$

the components of $\mathbf{A}_h\mathbf{u}_h$ can be bounded in $L^2(\mathcal{M})$ as follows

$$
\begin{aligned}
|A_{1h}\mathbf{u}_h|^2 &\le \Delta x\Delta y \sum_{i=1}^{3N_1}\sum_{j=1}^{3N_2}\left[\frac{3\tilde{u}_0^2}{\Delta x^2}|u_{i,j}-u_{i-1,j}|^2+\frac{3\tilde{v}_0^2}{\Delta y^2}|u_{i,j}-u_{i,j-1}|^2\right.\\
&\qquad\left.+\frac{3g^2}{\Delta x^2}|\phi_{i,j}-\phi_{i-1,j}|^2\right]\\
|A_{2h}\mathbf{u}_h|^2 &\le \Delta x\Delta y \sum_{i=1}^{3N_1}\sum_{j=1}^{3N_2}\left[\frac{3\tilde{u}_0^2}{\Delta x^2}|v_{i,j}-v_{i-1,j}|^2+\frac{3\tilde{v}_0^2}{\Delta y^2}|v_{i,j}-v_{i,j-1}|^2\right.\\
&\qquad\left.+\frac{3g^2}{\Delta x^2}|\phi_{i,j}-\phi_{i,j-1}|^2\right]\\
|A_{3h}\mathbf{u}_h|^2 &\le \Delta x\Delta y \sum_{i=1}^{3N_1}\sum_{j=1}^{3N_2}\left[\frac{4\tilde{u}_0^2}{\Delta x^2}|\phi_{i,j}-\phi_{i-1,j}|^2+\frac{4\tilde{v}_0^2}{\Delta y^2}|\phi_{i,j}-\phi_{i,j-1}|^2\right.\\
&\qquad\left.+4\tilde{\phi}_0^2\frac{|u_{i,j}-u_{i-1,j}|^2}{\Delta x^2}+4\tilde{\phi}_0^2\frac{|v_{i,j}-v_{i,j-1}|^2}{\Delta y^2}\right].
\end{aligned}
\tag{59}
$$

Next since

$$
|\mathbf{A}_h\mathbf{u}_h|^2=|A_{1h}\mathbf{u}_h|^2+|A_{2h}\mathbf{u}_h|^2+\frac{g}{\tilde{\phi}_0}|A_{3h}\mathbf{u}_h|^2,
$$

we infer readily from these inequalities that

$$
|\mathbf{A}_h\mathbf{u}_h|^2\le\kappa_2\sum_{i=1}^{3N_1}\sum_{j=1}^{3N_2}\left[\frac{\Delta y}{\Delta x}|\mathbf{u}_{i,j}-\mathbf{u}_{i-1,j}|^2+\frac{\Delta x}{\Delta y}|\mathbf{u}_{i,j}-\mathbf{u}_{i,j-1}|^2\right]
$$

where κ_2 depends on $\tilde{u}_0,\tilde{v}_0,\tilde{\phi}_0$ and g. □

We now introduce some coarse mesh consisting of the rectangles $K_{\lambda,\mu}, 1\le\lambda\le N_1, 1\le\mu\le N_2$:

$$
K_{\lambda,\mu}=\bigcup_{\alpha,\beta=0}^{2}k_{3\lambda-\alpha,3\mu-\beta}{}^2=\left(x_{3\lambda-2-1/2},x_{3\lambda+1/2}\right)\times\left(y_{3\mu-2-1/2},y_{3\mu+1/2}\right).
$$

We also define the fictitious rectangles $K_{0,\mu},K_{\lambda,0},\lambda=1,\dots N_1,\mu=1,\dots,N_2$, needed for the implementation of the boundary conditions; they are defined as above with μ or $\lambda=0$.

We introduce the space V_{3h} defined like V_h :

$$
\begin{aligned}
V_{3h}=\ &\{\text{step functions } w \text{ constant on } K_{\lambda,\mu},\ 0\le\lambda\le N_1,\ 0\le\mu\le N_2 \text{ with}\\
&\qquad w_{|K_{\lambda,\mu}}=w_{\lambda,\mu} \text{ and } w_{0,\mu}=w_{\lambda,0}=0\},
\end{aligned}
$$

and we set $\mathbf{V}_{3h}=(V_{3h})^3$.

If $\mathbf{u}_h\in\mathbf{V}_h$ and $\mathbf{u}_h|_{k_{ij}}=\mathbf{u}_{i,j}$, we define for $\lambda=1,\dots,N_1$ and $\mu=1,\dots,N_2$ the averages

$$
\mathbf{U}_{\lambda,\mu}=\frac{1}{9}\sum_{\alpha,\beta=0}^{2}\mathbf{u}_{3\lambda-\alpha,3\mu-\beta},
\tag{60}
$$

and the incremental unknowns

$$
\mathbf{Z}_{3\lambda-\alpha,3\mu-\beta}=\mathbf{u}_{3\lambda-\alpha,3\mu-\beta}-\mathbf{U}_{\lambda,\mu},
\tag{61}
$$

[2]Including, strictly speaking, the separation edges.

which satisfy of course

$$\sum_{\alpha,\beta=0}^{2} \mathbf{Z}_{3\lambda-\alpha,3\mu-\beta} = 0. \tag{62}$$

Let us denote by $(U_{\lambda,\mu}, V_{\lambda,\mu}, \Phi_{\lambda,\mu})$ the components of $\mathbf{U}_{\lambda,\mu}$ and by $(Z^u_{i,j}, Z^v_{i,j}, Z^\phi_{i,j})$ those of $\mathbf{Z}_{i,j}$. Also we define $\mathbf{U}_{3h}$ to be the step function equal to $\mathbf{U}_{\lambda,\mu}$ on $K_{\lambda,\mu}$ (on the coarse mesh) and let $\mathbf{Z}_h$ be the step function equal to $\mathbf{Z}_{i,j}$ on $k_{i,j}$ (on the fine mesh).

We note the following algebraic relations (using (62)):

$$\sum_{\alpha,\beta=0}^{2} |u_{3\lambda-\alpha,3\mu-\beta}|^2 = 9|U_{\lambda,\mu}|^2 + \sum_{\alpha,\beta=0}^{2} |Z^u_{3\lambda-\alpha,3\mu-\beta}|^2. \tag{63}$$

Multiplying by $\Delta x \Delta y$ and adding for $\lambda = 1, \ldots, N_1$ and $\mu = 1, \ldots, N_2$, we see that the L^2 norms of the corresponding step functions satisfy

$$|u_h|^2 = |U_{3h}|^2 + |Z^u_h|^2. \tag{64}$$

Since similar equalities hold for the other components we conclude that

$$|\mathbf{u}_h|^2 = |\mathbf{U}_{3h}|^2 + |\mathbf{Z}_h|^2 \tag{65}$$

where $|\cdot|$ is the norm in $\mathbf{H}$ associated to the scalar product (49).

3.3. Fully explicit Euler multilevel scheme and stability estimates. We will now proceed to some extent as in space dimension one. We define a time step Δt and we are given two integers $p > 1$ and $q > 1$. We will perform p steps with the small time step $\Delta t/p$ and the fine spatial mesh Δx, Δy and then we make q steps with the large time step Δt and the coarse spatial mesh $3\Delta x$, $3\Delta y$; and then we start again with the p steps.

The approximate solutions are recursively defined as follows. We start with the sequence $\mathbf{u}^0_h = (u^0_h, v^0_h, \phi^0_h)$ given by,

$$\begin{aligned} u^0_{i,j} &= \frac{1}{\Delta x \Delta y} \int_{k_{i,j}} u^0(x,y)dxdy, \\ v^0_{i,j} &= \frac{1}{\Delta x \Delta y} \int_{k_{i,j}} v^0(x,y)dxdy, \\ \phi^0_{i,j} &= \frac{1}{\Delta x \Delta y} \int_{k_{i,j}} \phi^0(x,y)dxdy, \end{aligned} \tag{66}$$

for $1 \le i \le 3N_1$, $1 \le j \le 3N_2$, where $\mathbf{u}^0$ is our initial condition, see (46).

Then using the Euler explicit scheme in time and with the definition of $\mathbf{A}_h$ introduced in (56), the discretization of (48) on the fine grid reads

$$\frac{p}{\Delta t}\left(\mathbf{u}_h^{n+(r+1)/p} - \mathbf{u}_h^{n+r/p}\right) + \mathbf{A}_h \mathbf{u}_h^{n+r/p} = 0. \tag{67}$$

Here, as for (13), n is a multiple of $(q+1)$ and $r = 0, \cdots, p-1$.

We first observe that

$$
\begin{aligned}
|u_h^0|^2 =& \sum_{i=1}^{N_1}\sum_{j=1}^{N_2} \Delta x\Delta y(|u_{i,j}^0|^2 + |v_{i,j}^0|^2 + \frac{g}{\tilde{\phi}_0}|\phi_{i,j}^0|^2) \\
=& \sum_{i=1}^{N_1}\sum_{j=1}^{N_2} \Delta x\Delta y \left[\left(\frac{1}{\Delta x\Delta y}\int_{k_{i,j}} u^0 dxdy \right)^2 \right. \\
& \left. + \left(\frac{1}{\Delta x\Delta y}\int_{k_{i,j}} v^0 dxdy \right)^2 + \frac{g}{\tilde{\phi}_0}\left(\frac{1}{\Delta x\Delta y}\int_{k_{i,j}} \phi^0 dxdy \right)^2 \right] \\
\leq& \text{(thanks to the Cauchy-Schwarz inequality)} \\
\leq& \sum_{i=1}^{N_1}\sum_{j=1}^{N_2} \left(\int_{k_{i,j}} (u^0)^2 dxdy + \int_{k_{i,j}} (v^0)^2 dxdy + \frac{g}{\tilde{\phi}_0}\int_{k_{i,j}} (\phi^0)^2 dxdy \right) \\
=& |\mathbf{u}^0|^2.
\end{aligned} \tag{68}
$$

Now, let us investigate the stability of the scheme (67). Taking the scalar product in $\mathbf{H}$ of (67) with $2\frac{\Delta t}{p}\mathbf{u}_h^{n+r/p}$, we obtain readily that

$$
2\langle \mathbf{u}_h^{n+(r+1)/p} - \mathbf{u}_h^{n+r/p}, \mathbf{u}_h^{n+r/p}\rangle + 2\frac{\Delta t}{p}\langle \mathbf{A}_h\mathbf{u}_h^{n+r/p}, \mathbf{u}_h^{n+r/p}\rangle = 0. \tag{69}
$$

Since

$$
2\langle \mathbf{u}_h^{n+(r+1)/p} - \mathbf{u}_h^{n+r/p}, \mathbf{u}_h^{n+r/p}\rangle = |\mathbf{u}_h^{n+(r+1)/p}|^2 - |\mathbf{u}_h^{n+r/p}|^2 - |\mathbf{u}_h^{n+(r+1)/p} - \mathbf{u}_h^{n+r/p}|^2, \tag{70}
$$

this gives :

$$
|\mathbf{u}_h^{n+(r+1)/p}|^2 - |\mathbf{u}_h^{n+(r+1)/p} - \mathbf{u}_h^{n+r/p}|^2 + 2\frac{\Delta t}{p}\langle \mathbf{A}_h\mathbf{u}_h^{n+r/p}, \mathbf{u}_h^{n+r/p}\rangle = |\mathbf{u}_h^{n+r/p}|^2. \tag{71}
$$

Lemma 3.1 provides the following lower bound :

$$
\begin{aligned}
2\frac{\Delta t}{p}\langle \mathbf{A}_h\mathbf{u}_h^{n+r/p}, \mathbf{u}_h^{n+r/p}\rangle \geq & 2\frac{\Delta t}{p}\kappa_1\Delta y \sum_{i=1}^{3N_1}\sum_{j=1}^{3N_2} \left| \mathbf{u}_{i,j}^{n+r/p} - \mathbf{u}_{i-1,j}^{n+r/p} \right|^2 \\
& + 2\frac{\Delta t}{p}\kappa_1\Delta x \sum_{i=1}^{3N_1}\sum_{j=1}^{3N_1} \left| \mathbf{u}_{i,j}^{n+r/p} - \mathbf{u}_{i,j-1}^{n+r/p} \right|^2 .
\end{aligned} \tag{72}
$$

Next we aim to estimate the term $|\mathbf{u}_h^{n+(r+1)/p} - \mathbf{u}_h^{n+r/p}|^2$. From equation (67) we have :

$$
\mathbf{u}_h^{n+(r+1)/p} - \mathbf{u}_h^{n+r/p} = -\frac{\Delta t}{p}\mathbf{A}_h\mathbf{u}_h^{n+r/p},
$$

and thanks to Lemma 3.2 we obtain that

$$
\begin{aligned}
|\mathbf{u}_h^{n+(r+1)/p} - \mathbf{u}_h^{n+r/p}|^2 \leq & \frac{\Delta t^2}{p^2}\kappa_2 \sum_{i=1}^{3N_1}\sum_{j=1}^{3N_2} \left[\frac{\Delta y}{\Delta x}|\mathbf{u}_{i,j}^{n+r/p} - \mathbf{u}_{i-1,j}^{n+r/p}|^2 \right. \\
& \left. + \frac{\Delta x}{\Delta y}|\mathbf{u}_{i,j}^{n+r/p} - \mathbf{u}_{i,j-1}^{n+r/p}|^2 \right].
\end{aligned} \tag{73}
$$

Combining estimates (73), (72) and (71) provides

$$
\begin{aligned}
|\mathbf{u}_h^{n+(r+1)/p}|^2 \; &+ \frac{\Delta y \Delta t}{p}\left[2\kappa_1 - \frac{\kappa_2 \Delta t}{p\Delta x}\right]\sum_{i=1}^{3N_1}\sum_{j=1}^{3N_2}|\mathbf{u}_{i,j}^{n+r/p} - \mathbf{u}_{i-1,j}^{n+r/p}|^2 \\
&+ \frac{\Delta x \Delta t}{p}\left[2\kappa_1 - \frac{\kappa_2 \Delta t}{p\Delta y}\right]\sum_{i=1}^{3N_1}\sum_{j=1}^{3N_2}|\mathbf{u}_{i,j}^{n+r/p} - \mathbf{u}_{i,j-1}^{n+r/p}|^2 \leq |\mathbf{u}_h^{n+r/p}|^2.
\end{aligned} \tag{74}
$$

We conclude that provided the following CFL conditions are satisfied :

$$
\frac{\kappa_2 \Delta t}{p\Delta x} \leq 2\kappa_1, \;\; \frac{\kappa_2 \Delta t}{p\Delta y} \leq 2\kappa_1,
$$

we have, for $r = 0, \cdots, p-1$,

$$
|\mathbf{u}_h^{n+(r+1)/p}| \leq |\mathbf{u}_h^{n+r/p}|. \tag{75}
$$

For the next q time-steps our approximate solutions take the form

$$
\mathbf{u}_h^{n+m+1} = \mathbf{U}_{3h}^{n+m+1} + \mathbf{Z}_h^{n+1}, \; m = 1, ..., q. \tag{76}
$$

The equation on the coarse grid reads

$$
\frac{1}{\Delta t}\left(\mathbf{U}_{3h}^{n+m+1} - \mathbf{U}_{3h}^{n+m}\right) + \mathbf{A}_{3h}\mathbf{U}_{3h}^{n+m} = 0, \;\; m = 1, \cdots, q. \tag{77}
$$

It is similar to (67) and, as above, by taking the scalar product in $\mathbf{H}$ of (77) with $2\Delta t \mathbf{U}_{3h}^{n+m}$ we can show that

$$
|\mathbf{U}_{3h}^{n+m+1}| \leq |\mathbf{U}_{3h}^{n+m}|, \;\; m = 1, \cdots, q, \tag{78}
$$

provided the following CFL conditions are satisfied :

$$
\frac{\kappa_2 \Delta t}{3\Delta x} \leq 2\kappa_1, \;\; \frac{\kappa_2 \Delta t}{3\Delta y} \leq 2\kappa_1.
$$

Returning to (76) and using (65), we then conclude that

$$
|\mathbf{u}_h^{n+m+1}| \leq |\mathbf{u}_h^{n+m}|, \; m = 1, ..., q. \tag{79}
$$

We have thus proven the following result.

Theorem 3.1. *The multilevel scheme defined by equations* (67) *and* (76)-(77) *is stable in* $L^\infty(0, +\infty, \mathbf{H})$ *provided the following CFL conditions are satisfied:*

$$
\frac{\Delta t}{\Delta x} \leq \frac{2\kappa_1}{\kappa_2}\min(3, p), \;\; \frac{\Delta t}{\Delta y} \leq \frac{2\kappa_1}{\kappa_2}\min(3, p). \tag{80}
$$

More precisely, for all n *and* $s \geq 0$*, the following bounds hold true*

$$
\begin{aligned}
&|\mathbf{u}_h^n| \leq |\mathbf{u}^0|, \\
&|\mathbf{u}_h^{s(q+1)+r/p}| \leq |\mathbf{u}^0|, \text{ for } r = 1, \cdots, p.
\end{aligned} \tag{81}
$$

Remark 3.1. *In the two-dimensional case we also note that for* $p = 1, 2$ *the CFL condition for* (77) *on the coarse grid is less restrictive than the one for* (67) *on the fine grid. For* $p = 3$ *the two CFL conditions are identical. For* $p > 3$ *the CFL condition on the coarse mesh is more restrictive than the one on the fine mesh. As done before a possible alternative is to use an Euler implicit scheme on the fine mesh and an Euler explicit scheme on the coarse mesh.*

4. Averaged Multilevel Finite Volume Method I

This section is devoted to another version of the multilevel finite volume method, the Averaged Finite Volume Method (AFVM) which is more efficient than the Hierarchical Finite Volume Method (HFVM) as the numerical simulations reported below will show. Interestingly however the proof of the stability of the method is not complete for both the implicit and explicit versions of this method. Other versions of the AFVM were implemented in [2] and studied in [5].

4.1. AFVM for the one dimensional advection equation. We consider again the one dimensional advection equation

$$\frac{\partial u}{\partial t}(x,t) + \frac{\partial u}{\partial x}(x,t) = 0, \quad (x,t) \in (0,L) \times (0,T), \tag{82}$$

supplemented with the boundary and initial conditions

$$u(0,t) = 0, \quad u(x,0) = u^0(x), \tag{83}$$

with $u^0 \in L^2(0,L)$.

Similarly to Section 2, we first introduce the fine cells $(k_i)_{1\le i\le 3N}$ of length Δx and the corresponding semi-discrete equations

$$\frac{du_i}{dt}(t) + \frac{u_i(t) - u_{i-1}(t)}{\Delta x} = 0, \quad 1 \le i \le 3N. \tag{84}$$

Then the coarse cells $(K_l)_{1\le l\le N}$ of length $3\Delta x$ are given by

$$K_l = k_{3l-2} \cup k_{3l-1} \cup k_{3l}, \quad 1 \le l \le N. \tag{85}$$

The coarse variables U_l and the increments Z_i in the AVFM are defined in the same way as in the HFVM that is

$$U_l = \frac{1}{3}\sum_{\alpha=0}^{2} u_{3l-\alpha}, \quad Z_{3l-\alpha} = u_{3l-\alpha} - U_l, \quad \alpha = 0,1,2. \tag{86}$$

Now we introduce the averaged multilevel (AFVM) method. The difference comes from the equation for U_l on the coarse mesh. Instead of applying the same scheme than the one on the fine mesh, we average the fine mesh schemes (84) on the three fine cells defining K_l and U_l, that is for $i = 3l, 3l-1, 3l-2$. This provides:

$$\frac{dU_l}{dt}(t) + \frac{u_{3l}(t) - u_{3l-3}(t)}{3\Delta x} = 0, \quad 1 \le l \le N, \tag{87}$$

or equivalently (compare to (11))

$$\frac{dU_l}{dt}(t) + \frac{U_l(t) - U_{l-1}(t)}{3\Delta x} + \frac{Z_{3l}(t) - Z_{3l-3}(t)}{3\Delta x} = 0, \quad 1 \le l \le N. \tag{88}$$

The AFVM can be found in [5] and [2].

For the fully discrete equations on the fine grid we use the Euler implicit scheme with time step $\Delta t/p$. Therefore we write for $1 \le i \le 3N$ and $0 \le r \le p-1$:

$$\begin{cases} \dfrac{u_i^{n+(r+1)/p} - u_i^{n+r/p}}{\Delta t/p} + \dfrac{u_i^{n+(r+1)/p} - u_{i-1}^{n+(r+1)/p}}{\Delta x} = 0, \\ u_0^{n+(r+1)/p} = 0. \end{cases} \tag{89}$$

This is the scheme we considered in Section 2.3 (see (35)) where we derived the following stability result in L^2 norm:

$$|u_h^{n+(r+1)/p}| \le |u_h^{n+r/p}|, \quad 0 \le r \le p-1. \tag{90}$$

Next we use the decomposition (86) and the increments Z_i are fixed during the computations on the coarse mesh so that our approximations read:

$$u_{3l-\alpha}^{n+m} = U_l^{n+m} + Z_{3l-\alpha}^{n+1}, \quad 1 \le l \le N, \quad \alpha = 0,1,2, \quad m = 1, \cdots, q+1. \tag{91}$$

On the coarse mesh we discretize in time the equation (87) using the Euler implicit scheme and the time step Δt. This provides:

$$\begin{cases} \dfrac{U_l^{n+m+1} - U_l^{n+m}}{\Delta t} + \dfrac{u_{3l}^{n+m+1} - u_{3l-3}^{n+m+1}}{3\Delta x} = 0, \quad m = 1, \cdots, q, \\ U_0^{n+m+1} = 0, \end{cases} \tag{92}$$

or equivalently

$$\frac{U_l^{n+m+1} - U_l^{n+m}}{\Delta t} + \frac{U_l^{n+m+1} - U_{l-1}^{n+m+1}}{3\Delta x} + \frac{Z_{3l}^{n+1} - Z_{3l-3}^{n+1}}{3\Delta x} = 0. \tag{93}$$

Remark 4.1. *In the above scheme since*

$$U_l^{n+m+1} - U_l^{n+m} = u_{3l}^{n+m+1} - u_{3l}^{n+m},$$

the equations (92), (93) *also read*

$$\frac{u_{3l}^{n+m+1} - u_{3l}^{n+m}}{\Delta t} + \frac{u_{3l}^{n+m+1} - u_{3l-3}^{n+m+1}}{3\Delta x} = 0. \tag{94}$$

If we multiply equation (94) *by* $2\Delta x \Delta t u_{3l}^{n+m+1}$, *we obtain*

$$\begin{aligned} &\Delta x \left[|u_{3l}^{n+m+1}|^2 - |u_{3l}^{n+m}|^2 + |u_{3l}^{n+m+1} - u_{3l}^{n+m}|^2 \right] \\ &+ \frac{\Delta t}{3} \left[|u_{3l}^{n+m+1}|^2 - |u_{3l-3}^{n+m+1}|^2 + |u_{3l}^{n+m+1} - u_{3l-3}^{n+m+1}|^2 \right] = 0. \end{aligned} \tag{95}$$

By summing for $l = 1, \cdots, N$, *we find*

$$\begin{aligned} &|u_{3h}^{n+m+1}|^2 - |u_{3h}^{n+m}|^2 + \Delta x \sum_{l=1}^{N} |u_{3l}^{n+m+1} - u_{3l}^{n+m}|^2 \\ &+ \frac{\Delta t}{3} \left[|u_{3N}^{n+m+1}|^2 + \sum_{l=1}^{N} |u_{3l}^{n+m+1} - u_{3l-3}^{n+m+1}|^2 \right] = 0, \end{aligned} \tag{96}$$

where for $\tau = n+m+1, n+m$, *we used the following notation*

$$|u_{3h-\alpha}^{\tau}|^2 = \Delta x \sum_{l=1}^{N} |u_{3l-\alpha}^{\tau}|^2, \quad \alpha = 0,1,2. \tag{97}$$

We derive from (96) *the following estimates*

$$|u_{3h}^{n+m+1}| \le |u_{3h}^{n+m}|. \tag{98}$$

We would then need the estimates for $|u_{3h-\alpha}^{n+r+1}|$, $\alpha = 1,2$, *which are not available.*

4.2. Spectral analysis. In this section we return to the stability study performed in Section 4 of [5]; this study is not bending and partly withdrawn as explained below. The equation under consideration is again the advection equation

$$\frac{\partial u}{\partial t} + \frac{\partial u}{\partial x} = 0, \quad \text{in } (0, L) \times (0, T), \tag{99}$$

but it is now supplemented with the space periodicity boundary condition:

$$u(0, t) = u(L, t), \tag{100}$$

together with some initial data $u_0 \in L^2(0, L)$.

As in Section 4.1, we can discretize the above problem by using the AFVM. In view of the new boundary condition, the scheme on the fine grid now reads:

$$\begin{cases} \dfrac{u_i^{n+(r+1)/p} - u_i^{n+r/p}}{\Delta t/p} + \dfrac{u_i^{n+(r+1)/p} - u_{i-1}^{n+(r+1)/p}}{\Delta x} = 0, \\ u_0^{n+(r+1)/p} = u_{3N}^{n+(r+1)/p}, \end{cases} \tag{101}$$

for $1 \le i \le 3N$ and $0 \le r \le p-1$.

We associate with a periodic sequence v_i, $i \in \mathbb{Z}$, $v_{i+3N} = v_i$, its discrete Fourier coefficients (see [7]) defined as follows:

$$\hat{v}_j = \frac{1}{3N} \sum_{k=1}^{3N} e^{-ijkh^*} v_k, \ \ j = 1, \dots, 3N, \tag{102}$$

where $h^* = \frac{2\pi}{3N}$. The stability analysis made by the Von Neumann method (see [5] and e.g. [19]) gives:

$$|u_h^{n+(r+1)/p}| \le |u_h^{n+r/p}|, \ \ 0 \le r \le p-1. \tag{103}$$

Now the averaged multilevel finite volume scheme on the coarse mesh reads:

$$\begin{cases} \dfrac{U_l^{n+m+1} - U_l^{n+m}}{\Delta t} + \dfrac{u_{3l}^{n+m+1} - u_{3l-3}^{n+m+1}}{3\Delta x} = 0, \ \ m = 1, \cdots, q \\ U_0^{n+m+1} = U_N^{n+m+1}, \end{cases} \tag{104}$$

and the approximations are given by

$$u_{3l-\alpha}^{n+m} = U_l^{n+m} + Z_{3l-\alpha}^{n+1}, \ \ 1 \le l \le N, \ \ \alpha = 0, 1, 2. \tag{105}$$

Since the Z are fixed while performing the coarse mesh calculations we see that

$$U_l^{n+m+1} - U_l^{n+m} = u_{3\ell-\alpha}^{n+m+1} - u_{3\ell-\alpha}^{n+m}, \ \ \alpha = 0, 1, 2.$$

In view of this equality for $\alpha = 0$, (104) becomes

$$\frac{1}{\Delta t}(u_{3l}^{n+m+1} - u_{3l}^{n+m}) + \frac{1}{3\Delta x}(u_{3l}^{n+m+1} - u_{3l-3}^{n+m+1}) = 0, \tag{106}$$

that is,

$$\left(1 + \frac{\Delta t}{3\Delta x}\right) u_{3l}^{n+m+1} - \frac{\Delta t}{3\Delta x} u_{3l-3}^{n+m+1} = u_{3l}^{n+m}. \tag{107}$$

Returning to the definition of the discrete Fourier coefficients associated with a periodic sequence v_i, $v_{i+3N} = v_i$, we write, for $j = 1, \ldots, 3N$:

$$\begin{aligned}\hat{v}_j &= \frac{1}{3N}\sum_{k=1}^{3N} v_k e^{-ih^*kj} \\ &= \frac{1}{3N}\sum_{\ell=1}^{N}\left(v_{3l}e^{-3ih^*lj} + v_{3l-1}e^{-ih^*(3l-1)j} + v_{3l-2}e^{-ih^*(3l-2)j}\right).\end{aligned}$$

We now introduce the partial Fourier sum :

$$\hat{v}_{(3l-\alpha),j} = \frac{1}{3N}\sum_{\ell=1}^{N} v_{3l-\alpha}e^{-ih^*3lj}, \;\; j = 1, \ldots, 3N. \tag{108}$$

We observe that this partial Fourier sum is periodic in j with period $3N$ and that the Parseval relation holds in the form :

$$\sum_{j=1}^{3N}|\hat{v}_{(3l-\alpha),j}|^2 = \frac{1}{3N}\sum_{\ell=1}^{N}|v_{3l-\alpha}|^2, \;\; \alpha = 0, 1, 2. \tag{109}$$

We also have

$$\hat{v}_{(3l-3),j} = \hat{v}_{(3l),j}e^{-3ih^*j}. \tag{110}$$

With this definition in mind, we now take the partial Fourier transform of (107). This yields:

$$\left(1 + \frac{\Delta t}{3\Delta x}\right)\hat{u}^{n+m+1}_{(3l),j} - \frac{\Delta t}{3\Delta x}e^{-3ih^*j}\hat{u}^{n+m+1}_{(3l),j} = \hat{u}^{n+m}_{(3l),j}. \tag{111}$$

Hence

$$\hat{u}^{n+m+1}_{(3l),j} = g_{C,j}\hat{u}^{n+m}_{(3l),j}, \;\; j = 1, \ldots, 3N, \tag{112}$$

where the amplification factor $g_{C,j}$ on the coarse mesh is given by:

$$g^{-1}_{C,j} = 1 + \frac{\Delta t}{3\Delta x}\left(1 - e^{-3ih^*j}\right). \tag{113}$$

We can conclude as in [5] that $|g^{-1}_{C,j}| \geq 1$, this implies the "stability" of the scheme (106). Also note that

$$\hat{u}^{n+m+1}_{(3l),j} = g^m_{C,j}\hat{u}^{n+1}_{(3l),j}, \;\; j = 1, \ldots, 3N, \;\; m = 1, ..., q. \tag{114}$$

Now we look for the expressions of the $\hat{u}^{n+m+1}_{(3l-\alpha),j}$, $\alpha = 0, 1, 2$, in terms of the $\hat{u}^{n+1}_{(3l-\beta),j}$; that of $\hat{u}^{n+m+1}_{(3l),j}$ has been already found at this stage, see (114).

We have the following:

$$\hat{u}^{n+m+1}_{(3l),j} = g^m_{C,j}\hat{u}^{n+1}_{(3l),j}, \tag{115}$$

$$\hat{u}^{n+m+1}_{(3l-1),j} = (g^m_{C,j} - 1)\hat{u}^{n+1}_{(3l),j} + \hat{u}^{n+1}_{(3l-1),j}, \tag{116}$$

$$\hat{u}^{n+m+1}_{(3l-2),j} = (g^m_{C,j} - 1)\hat{u}^{n+1}_{(3l),j} + \hat{u}^{n+1}_{(3l-2),j}. \tag{117}$$

We rewrite these equations in matricial form:

$$\begin{pmatrix}\hat{u}^{n+m+1}_{(3l),j} \\ \hat{u}^{n+m+1}_{(3l-1),j} \\ \hat{u}^{n+m+1}_{(3l-2),j}\end{pmatrix} = G^{(m)}_{C,j}\begin{pmatrix}\hat{u}^{n+1}_{(3l),j} \\ \hat{u}^{n+1}_{(3l-1),j} \\ \hat{u}^{n+1}_{(3l-2),j}\end{pmatrix}, \;\; j = 1, \ldots, 3N, \tag{118}$$

$$G_{C,j}^{(m)} = \begin{pmatrix} g_{C,j}^m & 0 & 0 \\ g_{C,j}^m - 1 & 1 & 0 \\ g_{C,j}^m - 1 & 0 & 1 \end{pmatrix}.$$

Now let us drop the indices m, j and C and write $G = G_{C,j}^{(m)}$, $g = g_{C,j}^m$. In [5] we mistakenly required the stability conditions $\rho(G) \leq 1$ instead of $\rho(\bar{G}^T G) \leq 1$, and found that indeed $\rho(G) \leq 1$.

Concerning $\rho(\bar{G}^T G)$ we can observe that for $g \neq 1, 0$, this spectral radius is strictly greater than one. Indeed, we have

$$\bar{G}^T G = \begin{pmatrix} |g|^2 + 2|g-1|^2 & \overline{g} - 1 & \overline{g} - 1 \\ g - 1 & 1 & 0 \\ g - 1 & 0 & 1 \end{pmatrix}.$$

The characteristic polynomial of this matrix is given by:

$$\Phi(X) = (1 - X)\left[X^2 - X(1 + |g|^2 + 2|g-1|^2) + |g|^2\right]. \tag{119}$$

Setting $Q(X) = X^2 - X(1 + |g|^2 + 2|g-1|^2) + |g|^2$, we observe that $Q(0) = |g|^2 > 0$ and $Q(1) = -2|g-1|^2 < 0$. Hence the roots of Q are real and positive, with one root λ_2 greater than one and one root λ_3 less than one. Therefore we can not conclude the stability analysis with the above Von Neumann analysis.

We can compute the eigenvectors of G corresponding to the three eigenvalues $\lambda_1 = 1$, λ_2 and λ_3 which are respectively:

$$\begin{pmatrix} 0 \\ 1 \\ -1 \end{pmatrix}, \quad \begin{pmatrix} 1 \\ -\frac{g-1}{1-\lambda_2} \\ -\frac{g-1}{1-\lambda_2} \end{pmatrix}, \quad \begin{pmatrix} 1 \\ -\frac{g-1}{1-\lambda_3} \\ -\frac{g-1}{1-\lambda_3} \end{pmatrix}. \tag{120}$$

Note that unlike in the classical Von Neumann analysis the fact that $\lambda_2 > 1$ does not imply that this scheme is unstable because the vector to which $G = G_{C,j}^{(m)}$ is applied in the right-hand side of (118) is a very particular combination of the above eigenvectors and the calculations in Section 4.3 show that this (implicit) scheme is, in fact, computationally stable in the context of our numerical simulations.

4.3. Numerical tests. In this section we present some simulations on the advection equation (99)-(100) using the averaged multilevel level method and the Euler implicit scheme, that is the method presented in Section 4.2. Our aim is to show that this scheme is numerically stable.

To test the numerical stability, it is convenient to add a source term to equation (99), that is to introduce:

$$\frac{\partial u}{\partial t} + \frac{\partial u}{\partial x} = S. \tag{121}$$

We consider the following analytic solution:

$$u_{EX}(x,t) = \cos(2\pi x/L)\cos(2\pi t) \tag{122}$$

and compute the source term S so that u_{EX} is indeed a solution of (121)

Table 1 below shows the L^2 relative errors at $t = 0.1$ with $p = 5$ and $q = 4$. The errors are computed for different values of Δx and Δt in order to test the numerical stability.

The first table shows that for $\Delta t \leq 10^{-3}$ the error stays about the same so that the scheme remains stable. The second table shows that after $\Delta t \simeq 0.4$ the scheme is not stable. The AFVM with the Euler implicit scheme is numerically stable in this context for Δt smaller than about 0.4.

TABLE 1. L^2 relative errors at $t = 0.1$ using AVFM with the Euler implicit scheme for the advection equation.

Δt	$\Delta x = 0.11$	$\Delta x = 0.037$	$\Delta x = 0.012$
10^{-2}	0.0627	0.0414	0.0317
10^{-3}	0.0495	0.0265	0.0141
10^{-4}	0.0484	0.0266	0.0134
10^{-5}	0.0486	0.0266	0.0134

TABLE 2. L^2 relative errors at $t = 10$ using AVFM with the Euler implicit scheme for the advection equation.

Δt	$\Delta x = 0.11$	$\Delta x = 0.037$	$\Delta x = 0.012$
0.1	0.2300	0.1765	0.1358
0.2	1.0742	0.9096	0.8722
0.4	10.2922	10.9827	11.1690

5. Averaged Multilevel Finite Volume Method II

In this section we consider the Averaged Multilevel Finite Volume Method for the two-dimensional linear shallow water equations. This method has been presented in [5] and [2] and we first recall it in Section 5.1. We do not prove any stability result but we aim to compare the AFVM to the HFVM in the numerical simulations presented in Section 5.2.

5.1. AFVM for the linear shallow water equations with Euler explicit. The linear shallow water equations on the domain $\mathcal{M} = (0, L_1) \times (0, L_2)$ read (see (44))

$$\left\{ \begin{array}{l} \dfrac{\partial u}{\partial t} + \tilde{u}_0 \dfrac{\partial u}{\partial x} + \tilde{v}_0 \dfrac{\partial u}{\partial y} + g \dfrac{\partial \phi}{\partial x} = 0, \\ \dfrac{\partial v}{\partial t} + \tilde{u}_0 \dfrac{\partial v}{\partial x} + \tilde{v}_0 \dfrac{\partial v}{\partial y} + g \dfrac{\partial \phi}{\partial y} = 0, \\ \dfrac{\partial \phi}{\partial t} + \tilde{u}_0 \dfrac{\partial \phi}{\partial x} + \tilde{v}_0 \dfrac{\partial \phi}{\partial y} + \tilde{\phi}_0 \left(\dfrac{\partial u}{\partial x} + \dfrac{\partial v}{\partial y} \right) = 0. \end{array} \right. \tag{123}$$

We are still in the supercritical case, see (43), and we consider the boundary conditions:

$$u = v = \phi = 0 \text{ at } \{x = 0\} \cup \{y = 0\}. \tag{124}$$

The spatial discretization is similar to the one described in Section 3.2. We denote by $\mathbf{u}_h = (u_{i,j}, v_{i,j}, \phi_{i,j})$ the step function that approximates $\mathbf{u} = (u, v, \phi)$ on the fine mesh $k_{i,j}$.

In the AFVM, we first perform p time iterations on the fine mesh using the time step $\Delta t/p$ and the Euler explicit scheme. Setting for convenience $\tau = n + r/p$, the scheme reads:

$$\left\{ \begin{array}{l} \dfrac{u_h^{\tau+1/p} - u_h^\tau}{\Delta t/p} + \tilde{u}_0 \delta_h^1 u_h^\tau + \tilde{v}_0 \delta_h^2 u_h^\tau + g \delta_h^1 \phi_h^\tau = 0, \\ \dfrac{v_h^{\tau+1/p} - v_h^\tau}{\Delta t/p} + \tilde{u}_0 \delta_h^1 v_h^\tau + \tilde{v}_0 \delta_h^2 v_h^\tau + g \delta_h^2 \phi_h^\tau = 0, \\ \dfrac{\phi_h^{\tau+1/p} - \phi_h^\tau}{\Delta t/p} + \tilde{u}_0 \delta_h^1 \phi_h^\tau + \tilde{v}_0 \delta_h^2 \phi_h^\tau + \tilde{\phi}_0 (\delta_h^1 u_h^\tau + \delta_h^2 v_h^\tau) = 0, \end{array} \right. \tag{125}$$

where δ_h^1 and δ_h^2 are the discrete finite differences operator given by (54).

Next we introduce the decomposition of $\mathbf{u}_h$ as the sum of the coarse mesh averages $\mathbf{U}_{\lambda,\mu} = (U_{\lambda,\mu}, V_{\lambda,\mu}, \Phi_{\lambda,\mu})$ and the increments $\mathbf{Z}_{i,j}$ (see (60), (61)). Again the increments are fixed during the q iterations on the coarse grid so that:

$$\mathbf{u}_h^{n+m+1} = \mathbf{U}_{3h}^{n+m+1} + \mathbf{Z}_h^{n+1},\ m = 1, ..., q. \tag{126}$$

Then to obtain the equations for $\mathbf{U}_h$ on the coarse mesh, we average the equations (125) for $i = 3\lambda-2, 3\lambda-1, 3\lambda$ and $j = 3\mu-2, 3\mu-1, 3\mu$. To write down the scheme it is convenient to introduce the following discrete operators corresponding to the averages of the operators δ_h^1 and δ_h^2:

$$(\delta_{3h,h}^1 a_h)_{\lambda,\mu} = \sum_{j=3\mu-2}^{3\mu} \frac{1}{9\Delta x}(a_{3\lambda,j} - a_{3\lambda-3,j}),$$

$$(\delta_{3h,h}^2 a_h)_{\lambda,\mu} = \sum_{i=3\lambda-2}^{3\lambda} \frac{1}{9\Delta y}(a_{i,3\mu} - a_{i,3\mu-3}),$$

for $1 \le \lambda \le N_1$ and $1 \le \mu \le N_2$. Then the equations on the coarse grid read:

$$\begin{cases} \dfrac{U_h^{\tau+1} - U_h^\tau}{\Delta t} + \tilde{u}_0 \delta_{3h,h}^1 u_h^\tau + \tilde{v}_0 \delta_{3h,h}^2 u_h^\tau + g\delta_{3h,h}^1 \phi_h^\tau = 0, \\ \dfrac{V_h^{\tau+1} - V_h^\tau}{\Delta t} + \tilde{u}_0 \delta_{3h,h}^1 v_h^\tau + \tilde{v}_0 \delta_{3h,h}^2 v_h^\tau + g\delta_{3h,h}^2 \phi_h^\tau = 0, \\ \dfrac{\Phi_h^{\tau+1} - \Phi_h^\tau}{\Delta t} + \tilde{u}_0 \delta_{3h,h}^1 \phi_h^\tau + \tilde{v}_0 \delta_{3h,h}^2 \phi_h^\tau + \tilde{\phi}_0 \left(\delta_{3h,h}^1 u_h^\tau + \delta_{3h,h}^2 v_h^\tau\right) = 0, \end{cases} \tag{127}$$

where we have set $\tau = n + m$, $m = 1, ..., q$.

5.2. Numerical results. We aim to compare four different simulations for (123)-(124): one on the coarse mesh, one on the fine mesh, one using the hierarchical multilevel method (HFVM), and one using the averaged multilevel method (AFVM). But this time we consider equations (123) in which we add source terms to allow more flexibility, and in particular tests on exact solutions:

$$\begin{cases} \dfrac{\partial u}{\partial t} + \tilde{u}_0 \dfrac{\partial u}{\partial x} + \tilde{v}_0 \dfrac{\partial u}{\partial y} + g\dfrac{\partial \phi}{\partial x} = S_u, \\ \dfrac{\partial v}{\partial t} + \tilde{u}_0 \dfrac{\partial v}{\partial x} + \tilde{v}_0 \dfrac{\partial v}{\partial y} + g\dfrac{\partial \phi}{\partial y} = S_v, \\ \dfrac{\partial \phi}{\partial t} + \tilde{u}_0 \dfrac{\partial \phi}{\partial x} + \tilde{v}_0 \dfrac{\partial \phi}{\partial y} + \tilde{\phi}_0 \left(\dfrac{\partial u}{\partial x} + \dfrac{\partial v}{\partial y}\right) = S_\phi, \end{cases} \tag{128}$$

with,

$$\tilde{u}_0 = 2,\ \ \tilde{v}_0 = 2,\ \ \tilde{\phi}_0 = 1,\ \ g = 1. \tag{129}$$

The source terms are computed using the analytic functions in (132) below. We note that $\tilde{u}_0$, $\tilde{v}_0$ and $\tilde{\phi}_0$ enforce the supercritical conditions (43).

We describe the four different methods we aim to compare numerically.

- The scheme on the fine grid of size h is the standard (one level) explicit discretization of the equations using the time step $\Delta t/p$:

$$\frac{\mathbf{u}_h^{n+1} - \mathbf{u}_h^n}{\Delta t/p} + \mathbf{A}_h \mathbf{u}_h^n = 0,\ \ n \ge 0, \tag{130}$$

  where $\mathbf{A}_h$ is the discrete operator given by (55).

- The scheme on the coarse grid (size $3h$) is the one level explicit discretization of the equations using the time step Δt:

$$\frac{\mathbf{u}_{3h}^{n+1} - \mathbf{u}_{3h}^{n}}{\Delta t} + \mathbf{A}_{3h}\mathbf{u}_{3h}^{n} = 0, \;\; n \geq 0. \tag{131}$$

- The hierarchical multilevel method (HFVM) is given by the combination of p iterations of (130) on the fine grid (see (67)) followed by q iterations of (131) on the coarse grid (see (77)), but now the approximations take into account the incremental unknowns $\mathbf{Z}$ and are given by (76).
- The averaged multilevel method (AFVM method) is given by the combination of p iterations of (130) on the fine grid (see (125)) followed by q iterations of (127) on the coarse grid during which the increments are frozen ; the approximations take into account the incremental unknowns $\mathbf{Z}$ and are given by (126).

  This averaged multilevel method, is called averaged because the equations on the coarse grid are determined by summing the equations on the fine grid on nine cells and hence averaging them. This method is supposed to be more accurate that the HFVM, but the stability analysis is harder to derive.

The parameters are chosen as follows. The domain for our simulation is $(0,9) \times (0,9)$. Also we take $N_1 = N_2 = 90$, $\Delta t = 10^{-6}$, $p = 5$, $q = 4$. For the simulation on the fine mesh we use 270×270 control volumes and the time step 0.2×10^{-6}, for the simulation on the coarse mesh we use 90×90 control volumes and the time step 10^{-6}. Note that in these calculations we choose a Δt very small, much smaller than required by the CFL stability condition because we want to evaluate the errors due to the multilevel spatial discretization and avoid interferences with the time discretization errors. The choice of p and q is arbitrary, if q is much greater than p the error with the multilevel method will be closer to the error on the coarse mesh but the computation will be faster than the one on the fine mesh.
We consider the following exact solutions:

$$\begin{aligned} &u_{EX}(x,y,t) = x^3y^3cos(2t\pi), \;\; v_{EX}(x,y,t) = \sin\left(\frac{2y\pi}{9}\right)\cos(2t\pi)x^3, \\ &\phi_{EX}(x,y,t) = \sin\left(\frac{2x\pi}{9}\right)\cos(2t\pi)y^3, \end{aligned} \tag{132}$$

from which we analytically infer the source terms in (128).
The table below shows the computing times for the four methods, starting from $t = 0$ and going to $t = 3 \cdot 10^{-5}$ on a single thread intel processor.

Scheme	Time of the computation (in s)
Coarse mesh	11.1
HFVM	112.3
AFVM	129
Fine mesh	478.5

From the above table we conclude that the multilevel method is much faster than the one level method on the fine mesh. We also note below that the AFVM method multilevel method is more accurate than the HFVM. Figures 1, 2 and 3 show the L^2 relative errors of our four different simulations. We see that the errors using the multilevel methods is intermediate between the errors for the calculations on the coarse mesh and the ones on the fine mesh. Our proposed multilevel methods do

what we would expect: they are substantially faster than doing the whole computation on the fine mesh and the error is between that on the coarse mesh and that on the fine mesh.

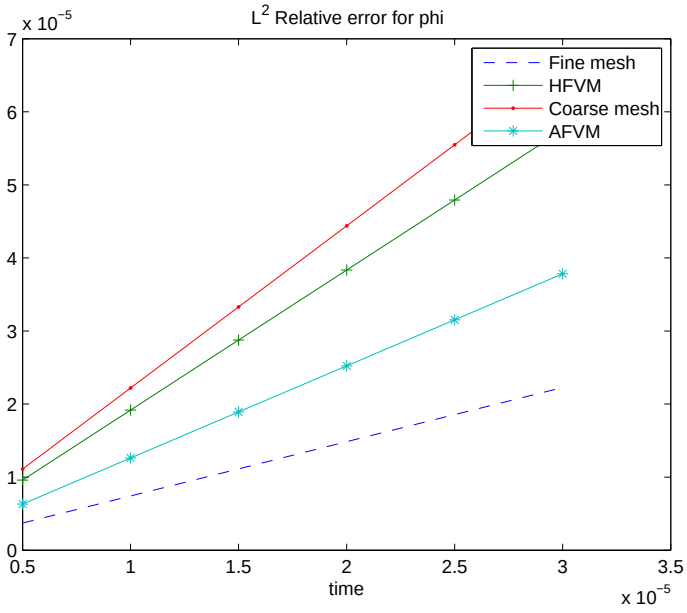

FIGURE 1. Relative L^2 error for ϕ using Euler explicit for the two dimensional linear shallow water equations

Acknowledgments.

This work was supported in part by the NSF Grant DMS 1206438, and by the Research Fund of Indiana University.

References

[1] R. Abgrall and S. Karni, Two-Layer Shallow Water Systems: A Relaxation Approach, *SIAM Journal on Scientific Computing*, 31, 2009, 1603–1627.

[2] K. Adamy, A. Bousquet, S. Faure, J. Laminie and R. Temam, A multilevel method for finite volume discretization of the two dimensional nonlinear shallow-water equations, *Ocean Modelling*, 33, 2010, 235–256.

[3] J. Balbas and S. Karni, A Central Scheme for Shallow Water Flows along Channels with Irregular Geometry, *Math. Model. Numer. Anal. (M2AN)*, 43, 2009, 333–351.

[4] A. Bousquet and A. Hung, Finite Volume Approximation of the Shallow Water Equations in Hyperbolic Mode, *in preparation.*

[5] A. Bousquet, M. Marion and R. Temam, Finite Volume Multilevel Approximation of the Shallow Water Equations, *Chinese Ann. Math*, 34B, 2013, 1–28.

[6] M.-O. Bristeau, B. Coussin, Boundary Conditions for the Shallow Water Equations solved by Kinetic Schemes, Rapport de recherche M3N - INRIA Rocquencourt, INRIA, 2006.

[7] C. Canuto, M. Y. Hussaini, A. Quarteroni and T. A. Zang, *Spectral methods. Evolution to complex geometries and applications to fluid dynamics,* Scientific Computation, Springer, Berlin, 2007.

[8] Q. Chen, M.-C. Shiue and R. Temam, The barotropic mode for the primitive equations, Special issue in memory of David Gottlieb, *Journal of Scientific Computing*, 45, 2010, 167–199.

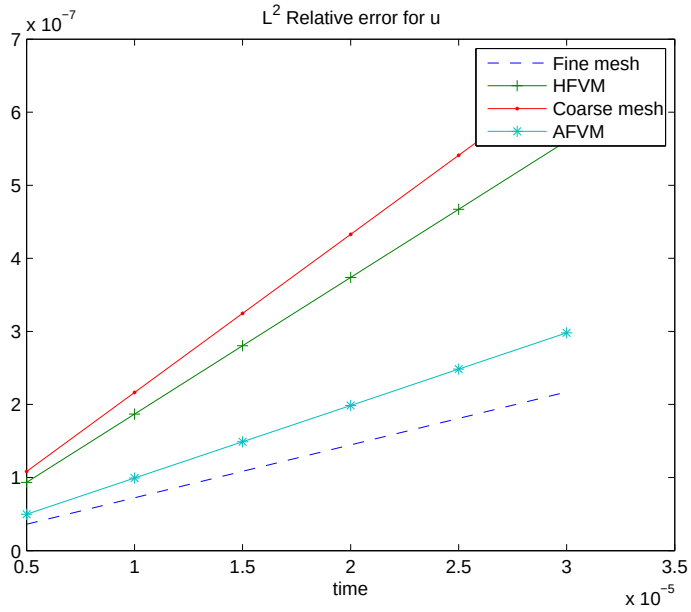

FIGURE 2. Relative L^2 error for u using Euler explicit for the two dimensional linear shallow water equations.

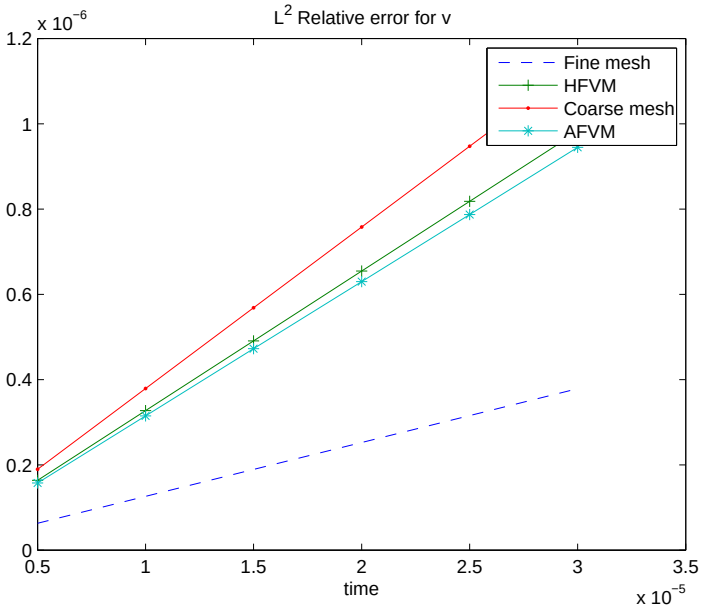

FIGURE 3. Relative L^2 error for v using Euler explicit for the two dimensional linear shallow water equations.

[9] Q. Chen, M.-C. Shiue, R. Temam and J. Tribbia, Numerical approximation of the inviscid 3D Primitive equations in a limited domain, *Math. Mod. and Num. Anal. (M2AN)*, 45, 2012, 619–646.

[10] G. Chiavassa and R. Donat, Numerical experiments with multilevel schemes for conservation laws, in *Godunov Methods* (Oxford, 1999), 155–160, Kluwer/Plenum, New York, 2001.
[11] T. Dubois, F. Jauberteau and R. Temam, *Dynamic multilevel methods and the numerical simulation of turbulence*, Cambridge University Press, Cambridge, 1999.
[12] G. Hernandez and S. Karni, Shallow Water Flows in Channels, *Journal of Scientific Computing*, Vol. 48, 2010, 190–208.
[13] A. Huang and R. Temam, The linearized 2d inviscid shallow water equations in a rectangle: boundary conditions and well-posedness, *Archive for Rational Mechanic and Analysis*, 2013, DOI 10.1007/s00205–013–0702–0.
[14] R. J. Leveque, *Finite Volume Methods for Hyperbolic Problems*, Cambridge Texts in Applied Mathematics, Cambridge University Press, 2002.
[15] M. Marion and R. Temam, Nonlinear Galerkin Methods, *SIAM J. Num. Anal.,* 26, 1989, 1139–1157.
[16] M. Marion and R. Temam, Navier-Stokes equations. Theory and Approximation. in *Handbook of Numerical Analysis*, P. G. Ciarlet and J. L. Lions, Eds. North-Holland, Amsterdam, Vol. VI, 1998, 503–689.
[17] R. Nair, S. Thomas and R. Loft, A Discontinuous Galerkin Global Shallow Water Model, *Mon. Wea. Rev.*, 133, 2005, 876-C888.
[18] A. Rousseau, R. Temam and J. Tribbia, The 3D Primitive Equations in the absence of viscosity: Boundary Conditions and well-posedness in the linearized case, *J. Math. Pures Appl.*, 89, 2008, 297–319.
[19] J. C. Strikwerda, *Finite difference schemes and partial differential equations*, SIAM, 2nd edition, 2004.
[20] R. Temam, Inertial manifolds and multigrid methods, *SIAM J. Math. Anal.*, 21, 1990, 154–178.
[21] R. Temam and J. Tribbia, Open boundary conditions for the primitive and Boussinesq equations, *J. of Atmospheric Sciences*, 60, 2003, 2647–2660.
[22] Chao Yang and Xiao-Chuan Cai, Parallel multilevel methods for implicit solution of shallow water equations with nonsmooth topography on the cubed-sphere, *J. Comput. Physics*, 230, 2011, 2523–2539.

The Institute for Scientific Computing and Applied Mathematics Indiana University, Bloomington, IN 47405, USA
E-mail: arthbous@indiana.edu
URL: http://mypage.iu.edu/∼arthbous
E-mail: mamarion@indiana.edu
E-mail: temam@indiana.edu
URL: http://mypage.iu.edu/∼temam/

Université de Lyon, Ecole Centrale de Lyon, CNRS UMR 5208, DMI 36 avenue Guy de Collongue, 69134 Ecully Cedex, France
E-mail: martine.marion@ec-lyon.fr